Demagnetizing fields in the de Haas–van Alphen effect*

G. W. Crabtree
Argonne National Laboratory, Argonne, Illinois 60439
(Received 14 February 1977)

A description of magnetic interaction, including demagnetizing effects and the vector nature of the magnetization, is presented. Demagnetizing factors appropriate for the second-order approximation for cubic and cylindrical sample shapes are explicitly calculated. A technique for measuring absolute amplitudes based on the weak interaction of two frequencies is proposed.

I. INTRODUCTION

Since it was first suggested by Shoenberg,[1] magnetic interaction has played an important role in understanding the amplitudes of the de Haas–van Alphen (dHvA) effect. Magnetic interaction (MI) of a single frequency with itself must be considered when cyclotron effective masses are derived from the temperature dependence of the amplitude, or when scattering lifetimes are derived from the field dependence of the amplitude.[2] Magnetic interaction of two frequencies often produces amplitude modulation of the higher frequency,[3,4] making interpretation of its amplitude difficult. Recently, magnetic interaction has been used as a tool for measuring properties which are otherwise difficult to determine: These include the absolute amplitude of the oscillation[5,6] and the sign of the second harmonic component of the signal.[7] Finally, demagnetizing effects have also been used experimentally to check whether the sample magnetization enters MI in a purely classical way or requires quantum-mechanical modification.[8]

In analyzing the effects of MI, it is often important to take into account the vector nature of the magnetization and the effect of the demagnetizing fields, both of which have received little attention in the literature. In this paper, an earlier derivation of MI[7] which includes these effects will be reviewed, and the demagnetizing effects for cylindrical and cubic sample shapes will be calculated explicitly. The details of the calculation are described in the text and a summary of the results is given at the end of the paper. In addition, comments on the effect of a field inhomogeneity in the presence of MI will be presented, and a technique for measuring absolute amplitudes using the magnetic interaction of two frequencies will be proposed.

II. MATHEMATICAL FORMULATION

The basic equations describing dHvA amplitudes in the presence of MI result from replacing the applied field $\vec{H}$ in the Lifshitz-Kosevich[9] (LK) expressions by the total field $\vec{B}$, where $\vec{B}$ includes contributions from the sample magnetization. The total field is given by

$$\vec{B}(\vec{r}) = \vec{B}_0 + 4\pi\vec{M}(\vec{r}) + \vec{b}(\vec{r}), \qquad (1a)$$

where $\vec{B}_0$ is the applied field assumed to be homogeneous, $\vec{M}(\vec{r})$ is the local magnetization of the sample at $\vec{r}$, and $\vec{b}(\vec{r})$ is the field produced at $\vec{r}$ by the distribution of magnetization $\vec{M}(\vec{r})$ throughout the sample. The latter term is referred to as the demagnetizing field, and is given by[10]

$$\vec{b}(\vec{r}) = -\nabla\left(\int_S \frac{\vec{M}(\vec{r})\cdot\hat{n}'}{|\vec{r}-\vec{r}'|}\,d^2r' - \int_V \frac{\vec{\nabla}'\cdot\vec{M}(\vec{r}')}{|\vec{r}-\vec{r}'|}\,d^3r'\right). \qquad (1b)$$

The first integral is over the surface and the second over the volume of the sample.

The LK expression for the oscillatory magnetization may be written[7,9]

$$\vec{M} = \vec{m}(\hat{H})\sum_{r=1}^{\infty} A_r \sin\left[2\pi r\left(\frac{F}{H}-\gamma\right)-\frac{p\pi}{4}\right], \qquad (2a)$$

$$\vec{m}(\hat{H}) = \hat{H} - \frac{1}{F}\frac{\partial F}{\partial\theta}\hat{\theta} - \frac{1}{F\sin\theta}\frac{\partial F}{\partial\phi}\hat{\phi}, \qquad (2b)$$

where $\vec{M}$ is the oscillatory magnetization, $F(\theta,\phi)$ is the frequency of oscillation in $1/H$ for the field direction $\hat{H}$ specified by the spherical coordinates (θ,ϕ), γ is the Onsager phase constant, $p = +1$ (-1) if the extremal area of the Fermi surface associated with the oscillations is maximum (minimum), and $\vec{m}$ is the vector direction of the magnetization. Expressions for the temperature and field dependence of the amplitudes of the harmonic components A_r will not be needed in what follows and are defined in the literature.[7,9]

Equations (1) and (2) completely describe MI for a single frequency if $\vec{B}$ is substituted for $\vec{H}$ in Eq. (2). Various iterative techniques for finding M as a function of the applied field B_0 are described in the literature.[2,3,7,11] The present work follows the method of Crabtree *et al.*,[7] which is based on the work of Phillips and Gold.[3] The amplitudes A_r are assumed to decrease rapidly with increasing r, so that the order of the approximation is given by the subscript r (i.e., A_1 is first order, A_2 and A_1^2 are second order, etc.). The lowest approximation, correct to first order, is

$$\vec{M}_1 = \vec{m}(B_0)\, A_1 \sin\left[2\pi\left(\frac{F(\hat{B}_0)}{|B_0|} - \gamma\right) - \frac{p\pi}{4}\right], \quad \vec{B}_1(\vec{r}) = \vec{B}_0 + 4\pi\vec{M}_1 + \vec{b}_1(\vec{r}), \tag{3}$$

where the $\vec{r}$ dependence arises from substituting $\vec{M}_1$ in Eq. (1b). Iterating once and keeping terms to second order,

$$\vec{M}_2(\vec{r}) = \vec{m}(\hat{B}_1)\left\{A_1 \sin\left[2\pi\left(\frac{F(\hat{B}_1)}{|B_1|} - \gamma\right) - \frac{p\pi}{4}\right] + A_2 \sin\left[4\pi\left(\frac{F(\hat{B}_1)}{|B_1|} - \gamma\right) - \frac{p\pi}{4}\right]\right\}, \tag{4}$$

$$\vec{B}_2(\vec{r}) = \vec{B}_0 + 4\pi\vec{M}_2(\vec{r}) + \vec{b}_2(\vec{r}).$$

For simplicity, we assume $\vec{B}_0$ lies in a symmetry plane of the crystal so that $\partial F/\partial\phi = 0$ in Eq. (2b), and that the sample shape has sufficient symmetry that $\vec{b}$ is coplanar with $\vec{B}_0$ and $\vec{M}$. (As shown below, this is always the case for cubic shapes, and will be true for cylindrical shapes if the cylinder axis lies in the same symmetry plane as $\vec{B}_0$.) Then $\vec{B}_1$, $\vec{M}_1$, and $\vec{b}_1$ are related as in Fig. 1, and $|\vec{B}_1|$ may be approximated to first order by

$$|B_1| = B_0[1 + (4\pi M_1^{\parallel} + b_1^{\parallel})/B_0],$$

where the superscript $\parallel$ refers to the component

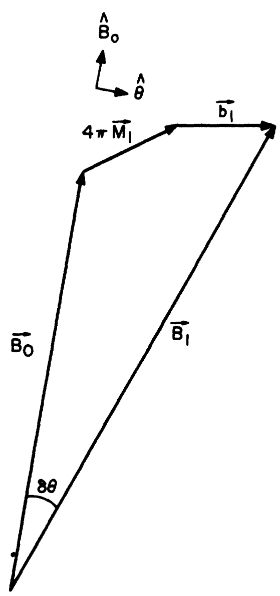

FIG. 1. Relation between $\vec{B}_0$, $\vec{M}_1$, $\vec{b}_1$, and $\vec{B}_1$. All four vectors are assumed to lie in a symmetry plane of the crystal (see text).

along $\hat{B}_0$ and $\perp$ will refer to the component along $\hat{\theta}$. With $\delta\theta$ defined in Fig. 1, $F(\hat{B}_1)$ may be approximated by

$$F(\hat{B}_1) = F(\hat{B}_0) + \frac{\partial F}{\partial\theta}\delta\theta = F(\hat{B}_0) + \frac{\partial F}{\partial\theta}\left(\frac{4\pi M_1^{\perp} + b_1^{\perp}}{B_0}\right).$$

Combining these approximations and keeping terms to first order,

$$\frac{F(\hat{B}_1)}{|B_1|} = \frac{F}{B_0^2}\left(\frac{1}{F}\frac{\partial F}{\partial\theta}(4\pi M_1^{\perp} + b_1^{\perp}) - (4\pi M_1^{\parallel} + b_1^{\parallel})\right), \tag{5}$$

where $F \equiv F(\hat{B}_0)$.

Note that $\vec{M}_1$ is uniform in space so that the volume term in (1b) does not contribute to $\vec{b}_1$. Also the surface term in Eq. (1b) is linear in $\vec{M}_1$, so that $\vec{b}_1(\vec{r})$ may be written

$$\vec{b}_1(\vec{r}) = -4\pi M_1^{\parallel}[I^{\parallel}(\vec{r})\hat{B}_0 + I^{\perp}(\vec{r})\hat{\theta}], \tag{6}$$

where

$$-4\pi M^{\parallel}\vec{I}(\vec{r}) \equiv \vec{\nabla}\int_S \frac{\vec{M}_1\cdot\hat{n}'}{|\vec{r} - \vec{r}'|}d^2r'.$$

This form will be convenient for showing the relation of this work to that of Phillips and Gold. Using

$$M^{\perp} = -\frac{1}{F}\frac{\partial F}{\partial\theta}M^{\parallel}$$

from Eq. (2b), Eq. (5) may be rewritten

$$2\pi F(\hat{B}_1)/B_1 = 2\pi F/B_0 - K(\vec{r})M_1^{\parallel}, \tag{7a}$$

where

$$K(\vec{r}) = \frac{8\pi^2 F}{B_0^2}\left[[1 - I^{\parallel}(\vec{r})] + \frac{1}{F}\frac{\partial F}{\partial\theta}\left(\frac{1}{F}\frac{\partial F}{\partial\theta} + I^{\perp}(\vec{r})\right)\right]. \tag{7b}$$

This approximation may be used to expand the sine functions in Eq. (4). Keeping terms to second order gives

$$\vec{M}_2(\vec{r}) = \vec{m}(\hat{B}_0)\{A_1 \sin[2\pi(F/B_0 - \gamma) - \tfrac{1}{4}p\pi] + A_2 \sin[4\pi(F/B_0 - \gamma) - \tfrac{1}{4}p\pi] - \tfrac{1}{2}K(\vec{r})A_1^2 \sin[4\pi(F/B_0 - \gamma) - \tfrac{1}{2}p\pi]\}, \tag{8}$$

where $\vec{B}_0$ may be substituted for $\vec{B}_1$ in the slowly varying functions $\vec{m}(\vec{B})$ and A_r. The first two terms are the usual LK fundamental and second harmonic, while the last term is an additional second harmonic due to magnetic interaction. The same technique can be applied to derive higher-order approximations; however, the volume term in Eq. (1b) will contribute to $\vec{b}(\vec{r})$ and the evaluation of $K(\vec{r})$ becomes more difficult. Much of the work using harmonic analysis of the dHvA effect deals with fundamental and second harmonics only, although recently work involving third harmonics has begun to appear.[12,13] In this paper, the approximation will not be carried past second order.

Equation (8) reduces to the result of Phillips and Gold if $K(\vec{r})$ is replaced by $8\pi^2F/B_0^2$. The term proportional to $(1/F)(\partial F/\partial\theta)$ inside the large square brackets of Eq. (7b) results from the vector nature of $\vec{M}$, while the terms in $I^{\parallel}(\vec{r})$ and $I^{\perp}(\vec{r})$ result from the demagnetizing field. $I^{\parallel}(\vec{r})$ and $I^{\perp}(\vec{r})$ play the role of local demagnetizing factors which describe the magnitude and direction of the demagnetizing field at $\vec{r}$.

The experimentally observed signal is proportional to $\int_V \vec{M}(\vec{r})d^3r$ where the integral is over the volume of the sample. The $\vec{r}$ dependence in Eq. (8) occurs only in $I^{\perp}(r)$ and $I^{\parallel}(r)$, so that the volume integral of $\vec{M}_2(\vec{r})$ is determined by the volume integral of $\vec{b}_1(r)$. Thus, demagnetizing effects correct to second order are completely determined by the volume integral of the first-order demagnetizing field. The following sections will calculate the volume integral of the first-order demagnetizing field for the case of cubic and cylindrical sample shapes. For ellipsoidal shapes $\vec{b}_1$ is constant over the volume of the sample and complete results are given by Osborne[14] and Stoner.[15]

III. CUBIC SHAPE

Using Eq. (1b), and letting $\vec{M}(\vec{r}) = \vec{M}_1 \equiv \vec{M}$, the desired integral is

$$\vec{b} \equiv \int_V \vec{b}(\vec{r})\, d^3r = -\int_V d^3r\, \vec{\nabla} \int_S d^2r' \frac{\vec{M}\cdot\hat{n}'}{|\vec{r}-\vec{r}'|}.$$

One integration over $\vec{r}$ may be done immediately:

$$b = -\int_S d^2r\, \hat{n} \int_S d^2r' \frac{\vec{M}\cdot\hat{n}'}{|\vec{r}-\vec{r}'|}. \quad (9)$$

With this expression, it may be shown that for the cube of side L, $\vec{b}\propto\vec{M}$. Consider the x component of Eq. (9), obtained by letting $\vec{r} = (\pm\frac{1}{2}L,\ y,\ z)$:

$$b_x = -\int_{-L/2}^{L/2} dy\, dz \int_S d^2r' \left(\frac{\vec{M}\cdot\hat{n}'}{[(\frac{1}{2}L - x')^2 + (y-y')^2 + (z-z')^2]^{1/2}} - \frac{\vec{M}\cdot\hat{n}'}{[(\frac{1}{2}L + x')^2 + (y-y')^2 + (z-z')^2]^{1/2}} \right).$$

The integration over r' has six contributions as r' falls on the six faces of the cube. For $\vec{r}' = (x', \pm\frac{1}{2}L, z')$ or $(x', y', \pm\frac{1}{2}L)$, the integrand is odd under the reflection $x' \to -x'$, forcing these contributions to vanish. For $\vec{r}' = (\pm\frac{1}{2}L, y', z')$ the surface integral is over y' and z', and b_x reduces to

$$b_x = -2M_x \int_{-L/2}^{L/2} dy\, dz \int_{-L/2}^{L/2} dy'\, dz' \left(\frac{1}{[(y-y')^2 + (z-z')^2]^{1/2}} - \frac{1}{[L^2 + (y-y')^2 + (z-z')^2]^{1/2}} \right). \quad (10)$$

Similar arguments hold for b_y and b_z where the integrals are the same for all three components by a change of variable. Transforming to the dimensionless variables y/L, z/L, y'/L, z'/L gives

$$\vec{b}/L^3 = -2k\vec{M}, \quad (11a)$$

$$k = \int_{-1/2}^{1/2} dy\, dz\, dy'\, dz' \left(\frac{1}{[(y-y')^2 + (z-z')^2]^{1/2}} - \frac{1}{[1 + (y-y')^2 + (z-z')^2]^{1/2}} \right). \quad (11b)$$

The value of k may be inferred by applying a sum rule derived by Schlomann.[16] The demagnetizing field for a uniformly magnetized body of arbitrary shape may be written

$$b_i(\vec{r}) = -4\pi \sum_k N_{ik}(\vec{r}) M_k,$$

where $N_{ik}(r)$ is a local demagnetizing tensor defined by

$$4\pi N_{ik}(\vec{r}) = \frac{\partial}{\partial x_i} \int \frac{\hat{x}_k\cdot\hat{n}'}{|\vec{r}-\vec{r}'|} d^2r'.$$

Schlomann has shown that

$$\sum_{i=1}^{3} N_{ii}(\vec{r}) = 1,$$

if $\vec{r}$ is inside the sample. Integration over the volume of the sample gives a similar sum rule for the average values of $N_{ii}(\vec{r})$. For the cube, the off-diagonal elements are zero and the diagonal elements are identical as shown by Eq. (11a). Thus $\int_V N_{ii}(\vec{r}) d^3r = \frac{1}{3}L^3$, and

$$\vec{b}/L^3 = -\tfrac{4}{3}\pi\vec{M}. \quad (12)$$

The integrals occurring in Eq. (11b) have been evaluated in the literature and give the same result.[17]

The average demagnetizing field is $-\frac{4}{3}\pi\vec{M}$, the same result as for the uniformly magnetized sphere. Since observed dHvA signals depend only on averages over the sample, the cube and the sphere are equivalent whenever the second-order approximation leading to Eq. (8) is valid. Specifically,

$$\int_V I^{\parallel}(\vec{r})\,d^3r = \tfrac{1}{3}V,$$

$$\int_V I^{\perp}(\vec{r})\,d^3r = -\tfrac{1}{3}V\frac{1}{F}\frac{\partial F}{\partial\theta}, \tag{13}$$

$$\int_V K(\vec{r})\,d^3r = \tfrac{2}{3}V\frac{8\pi^2 F}{B_0^2}\left[1+\left(\frac{1}{F}\frac{\partial F}{\partial\theta}\right)^2\right],$$

For either the sphere or the cube in the second-order approximation, where V is the volume of the sample.

The results in Eq. (13) are not restricted to the cube but apply to any sample with cubic symmetry. To see this, note that the derivation leading to Eq. (11a) used reflection symmetry of the sample shape through the xy, yz, and xz planes and cyclic changes of variable among (x, y, z). These properties are possessed by all shapes with cubic symmetry.

IV. CYLINDRICAL SHAPE

For a right circular cylinder of radius R and length L, we first evaluate

$$U(\vec{r}) \equiv \int_S \frac{\vec{M}\cdot\vec{n}'}{|\vec{r}-\vec{r}'|}\,d^2r'.$$

The function $1/(|\vec{r}-\vec{r}'|)$ may be expanded in Bessel functions[18] as

$$\frac{1}{|\vec{r}-\vec{r}'|} = \sum_{m=-\infty}^{\infty}\int_0^\infty dk\, e^{im(\phi-\phi')} \times J_m(k\rho)J_m(k\rho')e^{-k(z_>-z_<)},$$

where $(\rho,\ \phi,\ z)$ and $(\rho',\ \phi',\ z')$ represent $\vec{r}$ and $\vec{r}'$, respectively, in cylindrical coordinates. $z_>$ $(z_<)$ is the greater (lesser) of z and z'. Then

$$\begin{aligned} U(\mathrm{r}) = \int_0^R d\rho' \int_0^{2\pi} d\phi'\,\rho' M_z \Bigg(&\sum_{m=-\infty}^{\infty}\int_0^\infty dk\, e^{im(\phi-\phi')} J_m(k\rho)J_m(k\rho')e^{-k(\frac{1}{2}L-z)} \\ &- \sum_{m=-\infty}^{\infty}\int_0^\infty dk\, e^{im(\phi-\phi')} J_m(k\rho)J_m(k\rho')e^{-k(z+L/2)}\Bigg) \\ &+ \int_{-L/2}^{L/2} dz' \int_0^{2\pi} d\phi'\, R(M_x\cos\phi' + M_y\sin\phi') \sum_{m=-\infty}^{\infty}\int_0^\infty dk\, e^{im(\phi-\phi')} J_m(k\rho)J_m(kR)e^{-k(z_>-z_<)}. \end{aligned}$$

The first integral covers the end faces $z' = \pm\frac{1}{2}L$, the second covers the surface $\rho' = R$. Integration over ϕ' leaves only the $m=0$ term in the first integral and only $m=\pm1$ terms in the second. Integration over ρ' in the first integral is straightforward; integration over z' in the second must be broken into two ranges, $z'<z$ and $z'>z$. When these integrals are done,

$$\begin{aligned} U(\vec{r}) = {}& 4\pi R M_z \int_0^\infty \frac{dk}{k} J_0(k\rho)J_1(kR)e^{-kL/2}\sinh kz \\ &+ 4\pi R(M_x\cos\phi + M_y\sin\phi) \\ &\times \int_0^\infty \frac{dk}{k} J_1(k\rho)J_1(kR)(1-e^{-kL/2}\cosh kz). \end{aligned} \tag{14}$$

Local demagnetizing fields for the uniformly magnetized cylinder may be calculated from the above using $\vec{b}(\vec{r}) = -\vec{\nabla}U(\vec{r})$. To find the volume integral of $\vec{b}(\vec{r})$, Eq. (9) must be evaluated for the cylindrical geometry:

$$\begin{aligned} \vec{b} &= -\int_S d^2r\,\hat{n}U(\vec{r}) \\ &= -\hat{z}\int_0^R d\rho\int_0^{2\pi} d\phi\,\rho\left[U\left(\rho,\phi,\frac{L}{2}\right) - U\left(\rho,\phi,-\frac{L}{2}\right)\right] \\ &\quad - \int_{-L/2}^{L/2} dz\int_0^{2\pi} d\phi\, R(\hat{x}\cos\phi + \hat{y}\sin\phi)U(R,\ \phi,\ z). \end{aligned} \tag{15}$$

In the first term above, integration over ϕ removes the second term in Eq. (14). The first term in Eq. (14) may be integrated over ϕ and ρ to obtain

$$b_z = -16\pi^2R^2M_z\int_0^\infty \frac{dk}{k^2}J_1^2(kR)e^{-kL/2}\sinh k\frac{L}{2}. \tag{16}$$

In the second term of Eq. (15), the ϕ integration removes the first term of Eq. (14). The second term of Eq. (14) may be integrated over ϕ and z to obtain

$$-8\pi^2R^2\left(\frac{L}{2}\int_0^\infty \frac{dk}{k}J_1^2(kR)-\int_0^\infty \frac{dk}{k^2}J_1^2(kR)\times e^{-kL/2}\sinh k\frac{L}{2}\right)(\hat{y}M_y+\hat{x}M_x)\,.$$

Combining this with Eq. (16), rewriting the $\sinh(\frac{1}{2}kL)$ terms as exponentials, and using the integrals

$$\int_0^\infty \frac{J_1^2(x)}{x}dx=\tfrac{1}{2}\,,\quad \int_0^\infty \frac{J_1^2(x)}{x^2}dx=\frac{4}{3\pi}\,,$$

gives the result

$$\vec{b}=-\pi R^2L\left\{\hat{z}M_z4\pi\frac{2R}{L}\left(\frac{4}{3\pi}-\int_0^\infty\frac{dx}{x^2}J_1^2(x)e^{-(L/R)x}\right)+(\hat{x}M_x+\hat{y}M_y)2\pi\left[1-\frac{2R}{L}\left(\frac{4}{3\pi}-\int_0^\infty\frac{dx}{x^2}J_1^2(x)e^{-(L/R)x}\right)\right]\right\}. \tag{17}$$

Defining

$$D_z\left(\frac{L}{2R}\right)\equiv\left(\frac{4}{3\pi}-\int_0^\infty\frac{dx}{x^2}J_1^2(x)e^{-(L/R)x}\right)\frac{2R}{L}, \tag{18a}$$

$$D_\rho(L/2R)\equiv\tfrac{1}{2}[1-D_z(L/2R)]\,, \tag{18b}$$

Eq. (17) may be written

$$\vec{b}/\pi R^2L=-4\pi[\hat{z}M_zD_z(L/2R)+(\hat{x}M_x+\hat{y}M_y)D_\rho(L/2R)]\,. \tag{19}$$

This gives the average demagnetizing field for the uniformly magnetized cylinder. D_z and D_ρ are the average demagnetizing factors for the longitudinal and radial directions. The Bessel function integrals in the definitions of D_z and D_ρ cannot be done analytically, but numerical integration for a range of $L/2R$ values has been carried out by computer. The results are shown in Fig. 2 and Table I.

At $L/2R\simeq0.906$, the curves for D_ρ and D_z cross. Setting $D_\rho=D_z\equiv D$ in Eq. (18b) gives $D=\frac{1}{3}$. Therefore,

$$\vec{b}/2\pi R^2L=-\tfrac{4}{3}\pi\vec{M}\,,$$

in accordance with the sum rule derived by Schlomann. The average demagnetizing field is the same as in the sphere, and Eq. (13) gives the appropriate values for the volume integrals of $I^{\parallel}(\vec{r})$, $I^{\perp}(\vec{r})$, and $K(\vec{r})$.

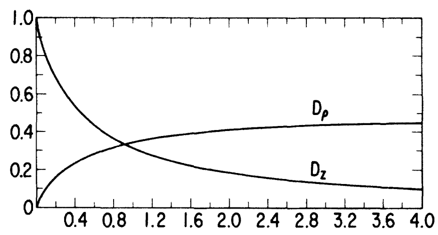

FIG. 2. Demagnetizing factors D_ρ and D_z as a function of the length to diameter ratio for a cylinder. The curves cross at $L/2R\simeq0.906$.

For other values of $L/2R$ the connection between Eq. (19) and the volume integrals is more complicated. In the coordinate system of Fig. 3, $\hat{B}_0$ and

TABLE I. Values of D_ρ and D_z from Eq. (8) for various values of $L/2R$.

$L/2R$	D_z	D_ρ	$L/2R$	D_z	D_ρ
0.0	1.000	0.000	3.1	0.123	0.438
0.1	0.796	0.101	3.2	0.120	0.439
0.2	0.680	0.159	3.3	0.116	0.441
0.3	0.594	0.202	3.4	0.113	0.443
0.4	0.528	0.235	3.5	0.110	0.444
0.5	0.474	0.262	3.6	0.107	0.446
0.6	0.430	0.284	3.7	0.105	0.447
0.7	0.393	0.303	3.8	0.102	0.448
0.8	0.361	0.319	3.9	0.100	0.449
0.9	0.334	0.332	4.0	0.0978	0.451
1.0	0.311	0.344	4.1	0.0956	0.452
1.1	0.291	0.354	4.2	0.0935	0.453
1.2	0.273	0.363	4.3	0.0914	0.454
1.3	0.257	0.371	4.4	0.0895	0.455
1.4	0.242	0.378	4.5	0.0876	0.456
1.5	0.230	0.384	4.6	0.0858	0.457
1.6	0.218	0.390	4.7	0.0841	0.457
1.7	0.207	0.396	4.8	0.0824	0.458
1.8	0.198	0.400	4.9	0.0808	0.459
1.9	0.189	0.405	5.0	0.0793	0.460
2.0	0.181	0.409	5.5	0.0723	0.463
2.1	0.174	0.412	6.0	0.0666	0.467
2.2	0.167	0.416	6.5	0.0616	0.470
2.3	0.161	0.419	7.0	0.0573	0.472
2.4	0.155	0.422	7.5	0.0536	0.473
2.5	0.149	0.425	8.0	0.0503	0.475
2.6	0.144	0.427	8.5	0.0473	0.476
2.7	0.140	0.429	9.0	0.0447	0.478
2.8	0.135	0.432	9.5	0.0424	0.479
2.9	0.131	0.434	10.0	0.0403	0.480
3.0	0.127	0.436			

the axis of the cylinder are assumed to lie in a symmetry plane of the crystal so that $\hat{B}_0$, $\hat{M}$, and $\hat{b}$ are coplanar. For convenience this is chosen to be the x-z plane. The angle between $\hat{B}_0$ and the cylinder axis is α, while θ (not shown in Fig. 3) may represent the angle of $\hat{B}_0$ with some other reference direction in the x-z plane, e.g., the direction of $\langle 100\rangle$. Using the transformations

$$M_z = M^{\parallel}\cos\alpha - M^{\perp}\sin\alpha\,,\quad M_x = M^{\parallel}\sin\alpha + M^{\perp}\cos\alpha \tag{20}$$

and

$$\hat{z} = \hat{B}_0\cos\alpha - \hat{\theta}\sin\alpha\,,\quad \hat{x} = \hat{B}_0\sin\alpha + \hat{\theta}\cos\alpha\,, \tag{21}$$

Eq. (19) may be written

$$\frac{\vec{b}}{\pi R^2 L} = -4\pi M^{\parallel}\left\{\left[\left(D_z\cos^2\alpha + D_\rho\sin^2\alpha - (D_\rho - D_z)\frac{1}{F}\frac{\partial F}{\partial\theta}\sin\alpha\cos\alpha\right)\right]\hat{B}_0 + \left[(D_\rho - D_z)\sin\alpha\cos\alpha - \frac{1}{F}\frac{\partial F}{\partial\theta}(D_z\sin^2\alpha + D_\rho\cos^2\alpha)\right]\hat{\theta}\right\}. \tag{22}$$

Using Eq. (6), the volume integrals of $I^{\parallel}(\vec{r})$ and $I^{\perp}(\vec{r})$ may be identified as the coefficients of $\hat{B}_0$ and $\hat{\theta}$ in large curly brackets above. These may be used in Eq. (7b) to find the volume integral of $K(\vec{r})$. The result is

$$\int_V K(\vec{r})\,d^3r = V\frac{8\pi^2 F}{B_0^2}\left[1 + \left(\frac{1}{F}\frac{\partial F}{\partial\theta}\right)^2 - D_\rho\left(\sin\alpha - \frac{1}{F}\frac{\partial F}{\partial\theta}\cos\alpha\right)^2 - D_z\left(\cos\alpha + \frac{1}{F}\frac{\partial F}{\partial\theta}\sin\alpha\right)^2\right].$$

V. INTERACTION OF TWO FREQUENCIES

In this section, a method for measuring absolute amplitudes when there is appreciable, but weak interaction between two dHvA frequencies, is discussed. The weak interaction expansion for the magnetic interaction expressions will be used and terms to second order will be kept. For simplicity, $\hat{B}_0$ is assumed parallel to a symmetry direction, so that $\partial F/\partial\theta = 0$ for both frequencies. Also the sample shape is assumed to have enough symmetry that $\hat{b}$ is parallel to $\hat{M}$. Then $\hat{B}_0$, $\hat{M}$, and $\hat{b}$ are parallel and the vector nature of the fields may be neglected. The equations to be iterated are

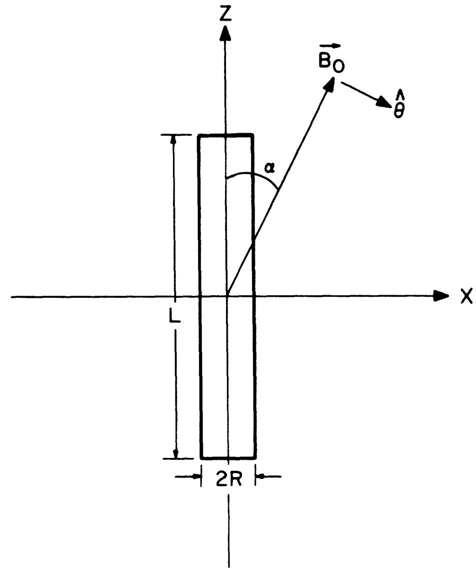

FIG. 3. Coordinate system used to relate D_ρ and D_z to $M^{\parallel}$ and $M^{\perp}$. $\vec{B}_0$ is chosen to lie in the x-z plane at an angle α to the cylinder axis. θ is the angle between $\vec{B}_0$ and an arbitrary reference direction in the x-z plane, e.g., the direction of $\langle 100\rangle$.

$$M = \sum_{r=1}^{\infty}\left\{A_r^a\sin\left[2\pi r\left(\frac{F_a}{B} - \gamma\right) - p_a\tfrac{1}{4}\pi\right] + A_r^b\sin\left[2\pi r\left(\frac{F_b}{B} - \gamma\right) - p_b\frac{\pi}{4}\right]\right\}, \tag{23}$$

$$B = B_0 + 4\pi M + b(\vec{r})\,,$$

where the indices a and b refer to the two frequencies. Iterating as before, and keeping terms to second order,

$$M = A_1^a\sin\left[2\pi\left(\frac{F_a}{B_0} - \gamma\right) - p_a\frac{\pi}{4}\right] + A_1^b\sin\left[2\pi\left(\frac{F_b}{B_0} - \gamma\right) - p_b\frac{\pi}{4}\right] + A_2^a\sin\left[4\pi\left(\frac{F_a}{B_0} - \gamma\right) - p_a\frac{\pi}{4}\right]$$
$$+ A_2^b\sin\left[4\pi\left(\frac{F_b}{B_0} - \gamma\right) - p_b\frac{\pi}{4}\right] - K_a(\vec{r})\frac{(A_1^a)^2}{2}\sin\left[4\pi\left(\frac{F_a}{B_0} - \gamma\right) - p_a\frac{\pi}{2}\right] - K_b(\vec{r})\frac{(A_1^b)^2}{2}\sin\left[4\pi\left(\frac{F_b}{B_0} - \gamma\right) - p_b\frac{\pi}{2}\right]$$
$$- \frac{A_1^a A_1^b}{2}(K_a + K_b)\sin\left[2\pi\left(\frac{F_a + F_b}{B_0} - 2\gamma\right) - (p_a + p_b)\frac{\pi}{4}\right] - \frac{A_1^a A_1^b}{2}(K_b - K_a)\sin\left[2\pi\left(\frac{F_a - F_b}{B_0}\right) - (p_a - p_b)\frac{\pi}{4}\right], \tag{24}$$

$$K_{a,b} = (8\pi^2/B_0^2)F_{a,b}[1 - I^{\parallel}(\vec{r})]\,.$$

This expansion is valid in the weak interaction limit, i.e., $K_a A_1^a$, $K_a A_1^b$, $K_b A_1^a$, and $K_b A_1^b \ll 1$. The first six terms are the usual Lifshitz-Kosevich and MI terms and the last two are sum and difference frequencies produced by "nonlinear mixing" via magnetic interaction.

The origin of the sum and difference sidebands may be understood in terms of frequency modulation. The oscillation F_a is frequency modulated by F_b, producing sidebands of amplitude $\pm \frac{1}{2} K_a A_1^a A_1^b$ at $F_a \pm F_b$. These sidebands have opposite sign as is usual for frequency modulation. Similarly, F_b is frequency modulated by F_a. However, if $F_a > F_b$, the sideband at $F_b - F_a$ appears at negative frequency. Inverting the frequency to $F_a - F_b$ to obtain a physically meaningful positive frequency causes a sign change in the amplitude of the side band because $\sin x$ is odd under the reflection $x \to -x$. After inversion, the sidebands of amplitude $\frac{1}{2} K_b A_1^a A_1^b$ appear at $F_a \pm F_b$ and have the same sign, which is characteristic of amplitude modulation (AM) of F_b by F_a. This demonstrates how frequency modulation (FM) of a lower frequency by a higher frequency appears as amplitude modulation of the higher frequency by the lower.

This type of "FM-AM effect" is in addition to that discussed by Alles and Lowndes.[4] They describe an instrumental effect due to the use of field modulation for observing the oscillations. In the present case, the amplitude modulation is inherent in the dHvA effect, independent of how the oscillations are observed.

This source of amplitude modulation is often overlooked in discussion of the dHvA waveshape in the presence of field inhomogeneity.[4,19] A complete treatment can be carried out as follows. The dHvA oscillations are first resolved into a spectrum of LK, MI, and combination terms as displayed above for weak interaction. The reduction in each term caused by field inhomogeneity may be found using the results of Hornfeldt, Ketterson, and Windmiller.[19] The resulting spectrum gives the inherent waveshape due to both MI and field inhomogeneity. (A similar scheme was recently proposed by Shoenberg for dealing with phase smearing due to crystal imperfections.[20]) If the oscillations are observed by field modulation, each term in the spectrum must be further weighted by the Bessel function appropriate for the frequency of the term and level of modulation. This Bessel function weighting accounts for the FM-AM effect described by Alles and Lowndes.

A well known case of AM due to MI is the neck-belly interaction in Au near ⟨111⟩.[4,11,20] In this case, the interaction is well outside the weak limit. This is graphically demonstrated in Fig. 4, where a Fourier transform of the belly signal at ⟨111⟩ is

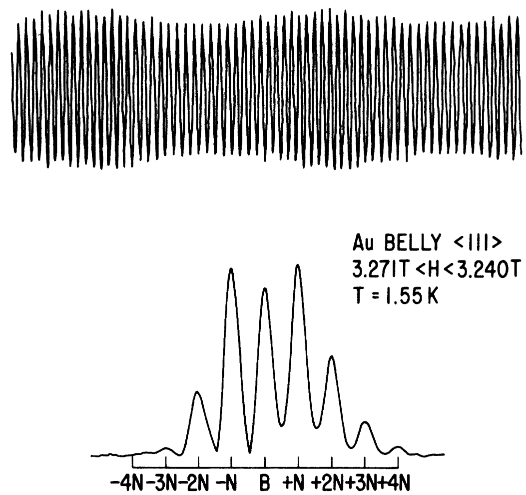

FIG. 4. Belly oscillations in Au for $\hat{B}_0$ along ⟨111⟩ in a sample of roughly cubic shape with an edge length of ~1 mm. The upper trace shows digitized data for part of a field sweep taken between 3.271 and 3.240 T at 1.55 K. The full sweep contained approximately 140 oscillations sampled about 7 times/oscillation. The choppy appearance is due to nonlinear pen motion between sampling points. The lower curve is the Fourier transform of the data showing the belly peak (B) and sidebands produced by magnetic interaction with the neck.

shown. Sidebands up to four neck frequencies away from the belly are evident. The interaction is so strong that the central peak at the frequency of the belly is appreciably reduced, and much of the power appears in the sidebands.

With such strong interaction, the analytical resolution of Eq. (23) into LK and combination terms is not practical, although a numerical solution could be carried out. [The problem is further complicated by the multivalued solutions of Eq. (23) for strong interaction,[11,21] which cause the sample to break into domains with different values of $\hat{M}$.[21]] Nevertheless, the contribution to AM of the belly caused by FM of the neck by the belly is of order $K_{\text{neck}} A_{\text{neck}}$ which is typically a few percent and may be treated by the weak interaction expansion. This small additional AM of the belly was not considered by Alles and Lowndes, and is of the right order of magnitude to explain discrepancies between the AM they observed and that caused by field modulation detection in a homogeneous field.

The expansion in Eq. (24) can also be used to measure the absolute amplitude of either of the interacting frequencies. If the amplitude of the sum or difference frequency is divided by one of the fundamental frequencies, one obtains, e.g., $\frac{1}{2} A_1^a (K_b \pm K_a)$, and A_1^a can be inferred if values for $K_{a,b}$ are taken from the first section of this work.

Because only ratios of measured amplitudes are used, the results are independent of the gain of the measuring system. This is a variation of a technique described by Randles[5] and developed by Alles, Higgins, and Lowndes,[6] where the MI contribution to the observed second harmonic is projected out and divided by the observed fundamental amplitude. In the present case, the interaction induced components occur at sum and difference frequencies and are automatically separated in frequency from the LK terms. Thus, it is not necessary to make the accurate phase measurements needed for separating the MI and LK contributions to the second harmonic. Furthermore, an important consistency check is available. The ratio of sum and difference amplitudes is $(F_a+F_b)/(F_b-F_a)$ independent of the gain of the system, demagnetizing factors, or Dingle temperatures. The ratio of sum and difference amplitudes thus gives a check on the field inhomogeneity and the validity of the weak interaction expansion.

One convenient test of this technique is the rosette-belly interaction for $\hat{H}$ along $\langle 100\rangle$ in Au. Fourier transforms of observed signals indicate the weak interaction limit is valid if the field and temperature are adjusted properly.[22] Absolute amplitudes for both orbits have been measured by other techniques and are available for comparison.[23,24]

VI. SUMMARY

The MI contribution to the dHvA wave shape is evaluated in second order in Eq. (8), taking into account both the local demagnetizing fields and the vector nature of the magnetization. For the cube and right circular cylinder with $L/2R \simeq 0.906$, the average demagnetizing field is independent of the direction of magnetization and the amplitude of the MI induced second harmonic is therefore independent of the orientation of the sample shape in the applied field. The value of $\int K(\vec{r})\,d^3r$ given in Eq. (13) may be used to calculate the amplitude of the MI induced second harmonic. For cylindrical samples with other values of $L/2R$, the average demagnetizing field depends explicitly on the angle α between the applied field and the cylinder axis. As a result, the amplitude of the MI-induced second harmonic also depends on α in a complicated and inconvenient way as described by Eq. (22) and the remarks following. Average demagnetizing factors for finite cylindrical sample shapes are given in Fig. 2 and Table I.

The magnetic interaction of two frequencies is examined in the weak interaction limit; the results are given in Eq. (24). The MI-induced sidebands appearing at the sum and difference frequencies are indicative of both frequency and amplitude modulation of the higher frequency by the lower. Since the sidebands are separated in frequency from the LK harmonics, their amplitudes may be measured directly without the need for any phase measurements. These amplitudes are a direct measure of the strength of the interaction and may be used to infer the absolute amplitude of either of the interacting frequencies if the demagnetizing factors are known. The technique cannot be applied to the neck-belly interaction in Au because the weak limit is far exceeded as shown in Fig. 4. However, the rosette and belly amplitudes near $\langle 100\rangle$ can be measured in this way if the field and temperature are properly adjusted.

ACKNOWLEDGMENT

The author would like to thank Professor J. B. Ketterson for helpful discussions and for reviewing the manuscript.

*Work supported under the auspices of the U. S. ERDA.

[1]D. Shoenberg, Philos. Trans. R. Soc. London Ser. A 255, 85 (1962).
[2]R. A. Phillips and A. V. Gold, Phys. Rev. 178, 932 (1969).
[3]D. Shoenberg, Can. J. Phys. 46, 1915 (1968).
[4]H. Alles and D. H. Lowndes, Phys. Rev. B 8, 5462 (1973).
[5]D. L. Randles, Proc. R. Soc. London Ser. A 331, 85 (1972).
[6]H. Alles, R. J. Higgins, and D. H. Lowndes, Phys. Rev. B 12, 1304 (1975).
[7]G. W. Crabtree, L. R. Windmiller, and J. B. Ketterson, J. Low Temp. Phys. 20, 655 (1975).
[8]P. M. Everett and C. G. Grenier, Bull. Am. Phys. Soc. 19, 250 (1974).
[9]I. M. Lifshitz and A. M. Kosevich, Zh. Eksp. Teor. Fiz. 29, 730 (1955) [Sov. Phys.-JETP 2, 636 (1956)].
[10]See, for example, J. R. Reitz and F. J. Milford, *Foundations of Electromagnetic Theory* (Addison-Wesley, Reading, Mass., 1960), Sec. 10-3.
[11]D. Shoenberg and J. J. Vuillemin, *Proceedings of the International Conference on Low Temperature Physics, Moscow*, 1966 (Nauka, Leningrad, 1966), p. 67.
[12]A. V. Gold and P. W. Schmor, Can. J. Phys. 54, 2445 (1977).
[13]Y. Chung, D. H. Lowndes, C. Lin Hendel, and J. P. Rode, Solid State Commun. 20, 101 (1976).
[14]J. A. Osborn, Phys. Rev. 67, 351 (1945).
[15]E. C. Stoner, Philos. Mag. 36, 803 (1945).
[16]E. Shlomann, J. Appl. Phys. 33, 2825 (1962).
[17]P. Rhodes and G. Rowlands, Proc. Leeds Philos. Lit. Soc. Sci. Sect. 6, 191 (1954).
[18]See, for example, J. D. Jackson, *Classical Electro-*

dynamics (Wiley, New York, 1962), problem 3.12.
[19]S. P. Hornfeldt, J. B. Ketterson, and L. R. Windmiller, J. Phys. E 6, 265 (1973).
[10]D. Shoenberg, J. Low Temp. Phys. 25, 755 (1976).
[21]J. H. Condon, Phys. Rev. 145, 526 (1966).
[22]G. Crabtree (unpublished).
[23]G. W. Crabteee, L. R. Windmiller, and J. B. Ketterson, J. Low Temp. Phys. 26, 755 (1977).
[24]M. Bibby and D. Shoenberg (unpublished).